Amorphous $Ni_{36}Zr_{35}Ti_{29}$ alloy as bipolar plates for polymer electrolyte membrane fuel cells

GY. THALMAIER[a], I. VIDA-SIMITI[a], H. VERMESAN[b], C. CODREAN[c], M. CHIRA[b]
[a]*Department of Materials Science and Engineering, Technical University of Cluj-Napoca, 103-105 Muncii Ave., 400641 Cluj-Napoca, Romania*
[b]*Department of Environmental Engineering and Sustainable Entrepreneurship, Technical University of Cluj-Napoca, 103-105 Muncii Ave., 400641Cluj-Napoca, Romania*
[c]*Department of Materials and Manufacturing Engineering, Politehnica University of Timisoara, 1 Mihai Viteazu Ave., 300222 Timisoara, Romania*

In this paper we are investigating the use of a $Ni_{36}Ti_{29}Zr_{35}$ amorphous material as a bipolar plate for polymer electrolyte membrane fuel cell (PEMFC). The amorphous material presents high corrosion resistance, mechanical strength and low interfacial contact resistance. The corrosion property of the present alloy has been investigated under conditions that simulate the fuel cell environment; hydrogen gas and air were bubbled into a 1 N H_2SO_4 solution at 70 °C. The studied amorphous alloy displayed a supercooled liquid region (~41K). The contact resistances measured on this amorphous alloy were found to be comparable with that of the uncoated 316L stainless steel and graphite.

(Received March 28, 2013; accepted July 11, 2013)

Keywords: Metallic glass, Bipolar plate, Polymer electrolyte fuel cell

1. Introduction

Polymer electrolyte membrane fuel cells (PEMFCs) are energy converters suitable for various applications with differing requirements. The obtained voltage per cell is small (~0.7V), in order to give useful voltages they have to be connected in series. The connection is made by using bipolar plate [1].

The ideal candidate material must possess low resistivity, high thermal conductivity, corrosion resistance, good mechanical properties, low hydrogen permeability, low- material costs and weight [2].

Two types of bipolar plates are studied as possible candidates carbon based and metal based materials. Graphite cannot be used to produce thin bipolar plates because of its brittleness and high manufacturing costs. Carbon composites are more suited to achieve the desired properties and permits manufacturing using well implemented mass production technologies [3].

Metallic bipolar plates could be an alternative. Stainless steels were employed in the early stages of developing bipolar plates [4]. Uncoated stainless steel is unsatisfactory mainly to insufficient corrosion resistance. Many different types of metallic bipolar plates have been developed based on stainless steels with different coatings [5-7]. Metals like Ta, Hf, Nb or Zr could have satisfactory corrosion resistance but they are much too costly to be considered a viable alternative. A great number of different, common alloys have been studied (Ti-based, Ni based, or Al alloys) but is the metal corrosion will cause poisoning of membrane or the catalyst [8]. Using an appropriate coating is mandatory [8].

Metallic glasses could also be considered as promising candidates since the compositions of metallic glasses are not restricted by the solubility limits, which allow the alloying of strong passivating elements within a wide composition range [9]. These alloys natively present excellent corrosion resistance and high metallic strength due to their structural and chemical homogeneity, there is no grain boundaries or other structural defects to aid corrosion. Furthermore, metallic glasses can show viscous flow deformation in a supercooled liquid state, which can aid the manufacturing process [10, 11].

E. Fleury et al. proposed the use of iron based metallic glass as bipolar plate. The plates have contact resistances similar to stainless steel and fracture strength of the order of 3GPa [12].

A number of nickel based amorphous alloys made of cheap, common metals were proposed to be used as bipolar plates. The potential of Ni–Nb–Ti–Zr metallic glasses for use in bipolar plates has previously been studied by Inoue et al. [13]. Some of this alloys have wide supercooled liquid regions of more than 60 K. The optimal composition from this point of view was found to be the alloy $Ni_{60}Nb_{15}Ti_{15}Zr_{10}$. The interfacial contact resistance and corrosion resistance of this alloy was further enhanced by carbon ion implantation by Kim et al. [14].Yoshioka et al. reported that Ni–Cr–P–B quaternary glassy alloys possess excellent corrosion resistance [15]. The alloy composition $Ni_{65}Cr_{15}P_{16}B_4$ from the same family can be melt-spun in air and that it had a supercooled liquid region of 43 K [16].

The present work investigates the possible use of an alloy of more simple composition ($Ni_{36}Ti_{29}Zr_{35}$ in at.%) as amorphous bipolar plate.

2. Experimental

The master alloy $Ni_{36}Ti_{29}Zr_{35}$ was prepared by arc melting using high purity metals in a Ti-gettered argon atmosphere. The alloys were melted several times in order to improve homogeneity. The alloy ingot was induction-melted under a high-purity argon atmosphere in a quartz crucible and injected through a nozzle onto a rotating Cu wheel to produce amorphous tapes. The surface speed of the copper roll used during the present experiments was 32 m/s. The obtained tapes were 3 mm wide and 60 µm thick and presented an amorphous structure. The amorphous nature of the ribbons was investigated with X-ray diffraction (Shimadzu XRD – 6000, λ=1,5418 Å, scanning at 2°/min, step 0.02°). Structural changes of the specimens upon heating were examined by differential scanning calorimetry (SETARAM Labsys system) at the heating rate of 20 K/min.

The corrosion behavior of the ribbons was investigated by electrochemical methods. Open circuit potential and potentiodynamic curves were used to analyze the corrosion characteristics of the amorphous samples. The experiments were carried out in a corrosion cell composed of the standard three-electrode arrangement in 1 N H_2SO_4 solution at 70 ºC bubbled with air and H_2. The specimen served as the working electrode, a platinum rod as counter electrode and a saturated Ag/AgCl electrode as reference electrode. The undesired areas the ribbons were sealed to prevent contact with the electrolyte.

Optical tensiometry was used to measure the water contact angle. The basis for optical tensiometry is the analysis of the shape of small drop water placed on the sample. The contact angle is determined by image analysis on the captured image.

Interfacial contact resistance (ICR) was approximated by the techniques developed by Davies [17] and Wang [18]. As current collectors gold plated copper plates are used and the gas diffusion layer was simulated by carbon paper. During the measurement the test specimen is covered on both sides by carbon paper and these are sandwiched between the current collectors.

Stress–strain curves were determined at room temperature using a Zwick/Roell Z005 tensile testing machine on an 80 mm-long, as obtained tape.

3. Results and discussions

Fig. 1. shows the XRD pattern of the as-quenched ribbons. Only a main halo peak without crystalline peaks is present, indicating a single glassy phase formed in these samples in the detection limit of the X-ray diffraction.

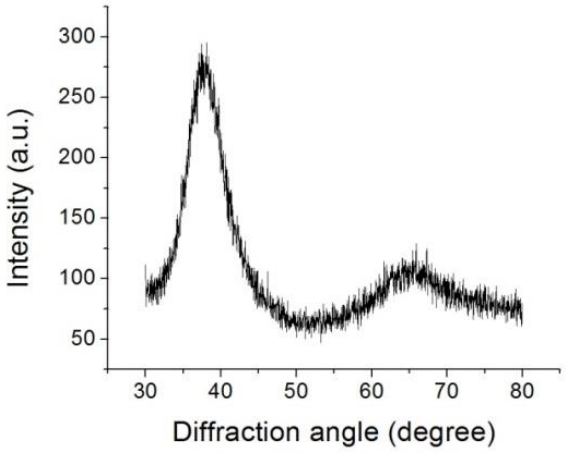

Fig. 1. XRD pattern of the $Ni_{36}Ti_{29}Zr_{35}$ *ribbons.*

The crystallization behavior of the obtained ribbons was studied using linear heating DSC experiments. On the DSC traces shown in Fig. 2, arrows indicate the glass transition temperature, T_g (at 316 ºC), and the first crystallization temperature, T_x (at 357 ºC). A second, more intense crystallisation peak can also be observed having an onset temperature of 489 ºC.

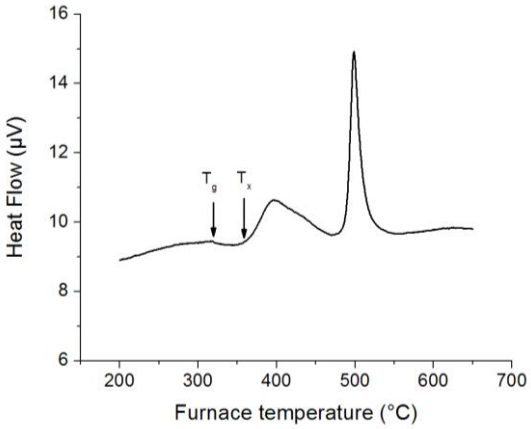

Fig. 2. DSC curve of the as-quenched Ni36Ti29Zr35 ribbons.

”

The studied alloy does not have the best glass forming ability, compared to the bulk metallic glasses, the reduced glass transition temperature ($T_r=T_g/T_m$) is around 0.4 compared to ~0.6 for the last. However, the DSC curve presents a supercooled region of 41ºC, which could permit forming in the supercooled liquid region.

Table 1. Thermal parameters of the present alloy.

Alloy	T_g (°C)	T_x (°C)	ΔT_x (°C)	T_m (°C)	T_r (°C)
$Ni_{36}Ti_{29}Zr_{35}$	316	357	41	841	0.39

In general, the electrical resistivity of the amorphous alloy is higher than that of its crystalline state because of the reduced mobility of the conduction electrons in the amorphous state. However, the contact resistance has a stronger influence on the cell performance than the bulk resistance of the bipolar plate [19].

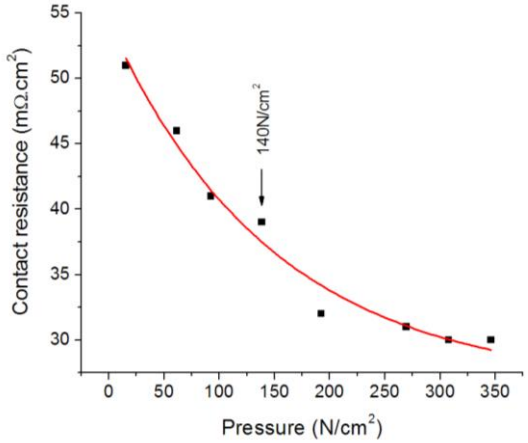

Fig. 3. Interfacial contact resistance measured at various compaction forces.

The contact resistance decreased with the increasing compaction force as shown in Fig. 3, which can be explained by the decrease of the interfacial resistance.

Table 2. ICR for different bipolar plate materials.

Alloy	ICR at 140N/cm^2 [mΩ*cm^2]
316L [20]	50
Graphite [21]	12
$Ni_{60}Nb_{20}Ti_{10}Zr_5Ta_5$ [19]	19
$Ni_{36}Ti_{29}Zr_{35}$	39

At stack assembly condition, about 140N/cm^2, the difference between the contact resistance of the amorphous alloys to the stainless steel and graphite is relatively small, indicating that this amorphous alloy can be applied as bipolar plates for PEMFC from the stand point of electrical properties.

In a polimer electrolite fuel cell, the bipolar plate is subjected to hydrogen rich corrosive environments in one side and oxygen rich in the other. In order to investigate the corrosion characteristics of the amorphous ribbons in the anode and cathode conditions, the potentiodynamic tests were done in H_2-containing and O_2-containing environments, respectively.

Fig. 4 presents the potentiodynamic curves in the H_2 and O_2 environments. Prior to the measurements the open circuit potential was monitored for 60 minutes to ensure constant potential.

Table 3. Polarization parameters at 70 ◦C in 1N H_2SO_4 bubbled with either air or H_2.

	E_{corr} (V)	i_{corr} (nA/cm^2)	Rp (Ωcm^2)	β_a (V)	β_c (V)
air	-158	28	996	165	-128
H_2	-245	46	209	205	-50

Comparing the two curves, we find that the corrosion potential of the alloy in the H_2SO_4 solution bubbled with air is higher than that in the solution bubbled with H_2, which is similar behavior as in the OCP tests (not presented in the present paper).

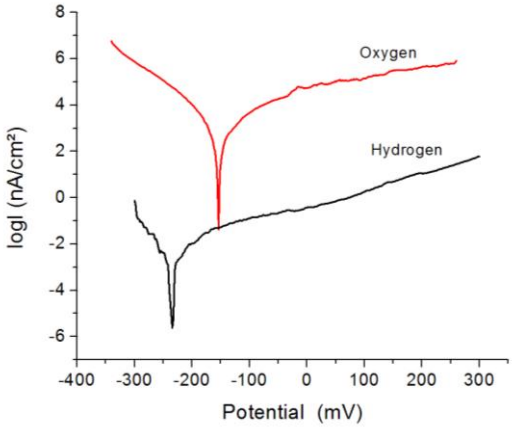

Fig. 4. Polarization curves at 70ºC in 1N H_2SO_4 bubbled with H_2 and O_2.

The increased corrosion potential retards corrosion in the oxygen-containing environment. Also, the corrosion current density is lower in the oxygen containing solution (28 nA/cm^2 vs 46 nA/cm^2). The high corrosion resistance can be explained by the high homogeneity of the ribbons which does not generate local preferential corrosion sites.

The water absorption at the cathodic part of the bipolar plate, which depends on the wettability of the material, affects the cell performance. If the generated water cannot be eliminated that part of the cell will be flooded and it's performance compromised [22]. In order to facilitate the water removal the wettability of the bipolar plate should be as low as posible, water contact angles higher than 90º are desired. The water contact angle of the present alloy (83º) is higher than that of the stainless steel (76º) but lower than that of the graphite (104º).

The mechanical behavior of the tapes was studied using stress-strain curves; such a curve is presented in Fig. 5. The obtained tapes present an elastic deformation (1.8%) and a tensile strength over 1100 MPa. The Young's modulus, defined as the ratio of the uniaxial stress over the uniaxial strain in the range of stress in which Hooke's law holds, is around 56.3 GPa.

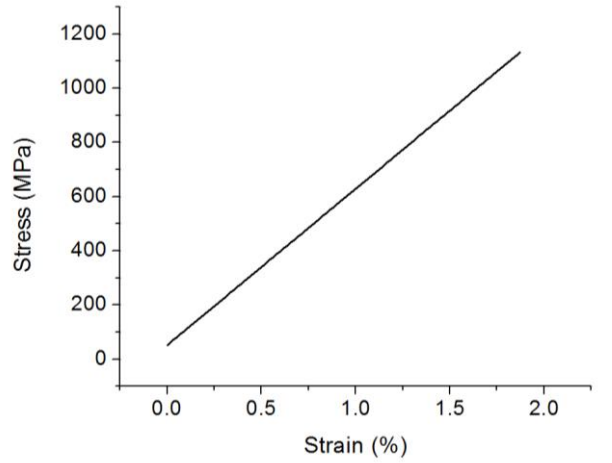

Fig. 5. Stress-strain curve of the studied alloy.

The high values of the mechanical properties can also be used advantageously since it allows a reduction of bipolar plate thickness while still providing high mechanical performance.

4. Conclusions

The properties of the $Ni_{36}Ti_{29}Zr_{35}$ alloy have been evaluated and compared with those of engineering materials proposed for bipolar plates.

The contact resistance of the present amorphous alloy was found to be comparable with that of 316L stainless steel and graphite. The corrosion resistance of the alloy according to the potentiodynamic curves is better than that of the 316L stainless steel. The corrosion resistance of the alloy in oxygen rich solution is higher than in the solution bubbled with hydrogen. The corrosion current is almost three times higher in the hydrogen rich atmosphere.

The high values of the mechanical properties can be used advantageously since it would allow the reduction of bipolar plate thickness to a minimum.

These results are encouraging for the possible application of this amorphous alloy as bipolar plates.

Acknowledgements

This paper was supported by the project "Development and support of multidisciplinary postdoctoral programmes in major technical areas of national strategy of Research - Development - Innovation" 4D-POSTDOC, contract no. POSDRU/89/1.5/S/52603, project co-funded by the European Social Fund through Sectorial Operational Programme Human Resources Development 2007-2013.

References

[1] J. Larminie, A. Dicks, Fuel Cell Systems Explained, second ed., John Wiley & Sons, West Sussex, 2003.
[2] N. M. Sammes, Fuel Cell Technology, Springer-Verlag, London, 2006
[3] R. A. Antunes, M. C. L. de Oliveira, G. Ett, V. Ett, J. Power Sources **196**, 2945 (2011).
[4] S. J. Lee, J. J. Lai, C. H. Huang. J. Power. Sources. **145**, 362 (2005).
[5] S. Joseph, J. C. McClure, R. Chianelli, P. Pich, P. J. Sebastian, Int. J. Hydrogen Energy **30**, 1339 (2005).
[6] S. J. Lee, C. H. Huang, Y. P. Chen, C. T. Hsu, J. Fuel Cell Sci. Technol. **2**, 290 (2005).
[7] H. Wang, J. A. Turner, J. Power Sources **170**, 387 (2007).
[8] R. A. Antunes, M. C. L. Oliveira, G. Ett, V. Ett, Int. J. Hydrogen Energy **35**, 3632 (2010).
[9] K. Hashimoto, P. Y. Park, J. H. Kim, H. Yoshioka, H. Mitsui, E. Akiyama, H. Habazaki, . Kawashima, K. Asami, Z. Grzesik, S. Mrowec, Mater. Sci. Eng. A, **198**, 1 (1995).
[10] R. Raicheff, V. Zaprianova, E. Gattef, J. Mater. Sci. Lett., **16**, 1701 (1997) .
[11] F. F. Marzo, A. R. Pierna, M. M. Vega, J. Non-Cryst. Solids, **329**, 108 (2003).
[12] E. Fleury, J. Jayaraj, Y. C. Kim, H. K. Seok, K. Y. Kim, K. B. Kim, Journal of Power Sources **159**, 34 (2006).
[13] A. Inoue, T. Shimizu, S. Yamaura, Y. Fujita, S. Takagi, H. M. Kimura, Mater. Trans. **46**, 1706 (2005).
[14] M. U. Kim, D. H. Kim, S.-H. Han, E. Fleury, H. K. Seok, P. R. Cha, Y. C. Kim, Met. Mater. Int., **17**, 283 (2011).
[15] H. Yoshioka, K. Asami, A. Kawashima, K. Hashimoto, Corros. Sci. **27**, 981 (1987).
[16] M. Yokoyama, S. Yamaura, H. M. Kimura, A. Inoue. Mater. Trans. **48**, 3176 (2007).
[17] D. P. Davies, P. L. Adcock, M. Turpin, S. J. Rowen, J. Appl. Electrochem. **30**, 101 (2000).
[18] H. Wang, M. A. Sweikart, J. A.Turner, J Power Sources **115**, 243 (2003).
[19] J. Jayaraj, Y. C. Kim, H. K. Seok, K. B. Kim, E. Fleury, Mater, Sci, Eng, A. **449-451**, 30 (2007).
[20] D. P. Davies, P. L. Adcock, M. Turpin, S. J. Rowen, J. Power Sources **86**, 237 (2000).
[21] W. Yoon, X. Huang, P. Fazzino, K. L. Reifsnider, M. A. Akkaoui, J. Power Sources **179**, 265 (2008).
[22] E. A Cho, U.-S Jeon, H. Y Ha, S.-A Hong, I.-H Oh, J. Power Sources, **125**, 178 (2004).

* Corresponding author: Gyorgy.Thalmaier@sim.utcluj.ro